3D MCSEM MODELING WITH COMSOL MULTIPHYSICS: A COMPARISON WITH OPEN-SOURCE SOFTWARE

Leandro Seabra ⓘ*, Higor Pires ⓘ, Watson Penha ⓘ,
Daniel Monteiro ⓘ, Antonio Monteiro ⓘ, and Victor Cezar Tocantins ⓘ

Universidade Federal do Pará - UFPA, Belém, PA, Brazil

*Corresponding author: leandro.seabra27@gmail.com

ABSTRACT. This work uses two approaches to present the numerical three-dimensional modeling of the MCSEM - Marine Controlled-Source Electromagnetic methods: the commercial software COMSOL Multiphysics and the open-source code `emg3d` for a theoretical model of resistive blocks. We first compare the results of the two methodologies through the electric field amplitude responses for three survey lines. We also analyze the necessary circumstances and boundary conditions for COMSOL Multiphysics to be used properly in the modeling. After this comparison, we explore the facilities of the model built into COMSOL Multiphysics and simulate the model for various frequencies with and without the presence of resistive bodies. Finally, we analyze the results and suggest lines of research for the construction of the simulations to be explored in numerical modeling in these two approaches. Thus, we ratify both approaches in their suitable domain, use, and importance through this work.

Keywords: electromagnetic; controlled-source; finite elements; Python.

INTRODUCTION

Large-scale modeling of 3D Controlled-Source Electromagnetic (CSEM) research and modeling are often a privilege for large companies and research consortia. This has changed in recent years and today there is a selection of different open-source codes available to everyone and also commercially licensed numerical modeling software accessible to teaching and research institutions. This work presents the numerical modeling in three dimensions (3D) of the MCSEM (Marine Controlled-Source Electromagnetic) method using two approaches: COMSOL Multiphysics commercial software and `emg3d` open-source code for a geophysical model formed by resistive blocks. Resistive blocks emulate a typical geological environment found in electromagnetic data acquisitions.

The use of marine resistivity/conductivity data from electrical and electromagnetic (EM) methods to understand the subsurface is not new. The adoption of onshore resistivity techniques and principles have been adapted to the marine environment since the early 1980s, as indicated by the works of Chave and Cox (1982, 1983). The improvement of techniques in data acquisition and in improvements in equipment and numerical codes opened new applications in various scenarios (Constable, 1990; Chave et al., 1991). Since the early 2000s, the works of Eidesmo et al. (2002) and Ellingsrud et al. (2002) have become major propagators of the method in the exploration of hydrocarbons in the service industry for large oil companies.

The MCSEM method is a tool great prominence in the exploration of hydrocarbons in deep and ultra-deep waters (Edwards, 2005). Basically, the MCSEM method uses a mobile horizontal electric dipole (HED) source near the sea floor and an array of electromagnetic field receivers deposited on the ocean floor, as illustrated in Figure 1. The electric dipole transmits a low frequency electromagnetic signal, from tenths to a few units of Hertz, energizing the layers of the seafloor. The diffusion of electromagnetic energy occurs in all directions of the water column and subsurface.

The signal detected in the receiver arrays is a combination of EM energy transmitted directly between the transmitter and receiver of EM energy reflected and refracted by the sea, air and seafloor layers of interest, notably the hydrocarbon reservoirs. (Fig. 1).
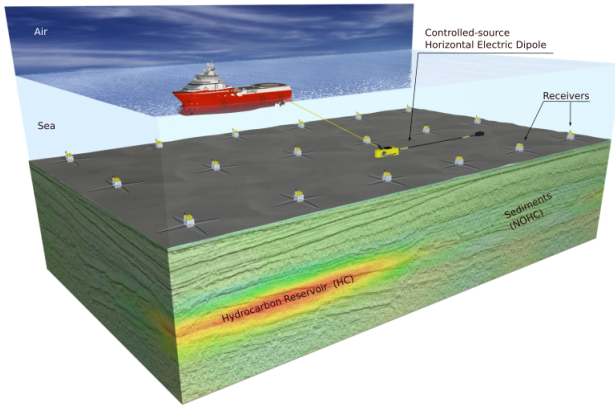

Figure 1: Illustrative representation of the MCSEM method. (Adapted from EMGS, 2022).

COMSOL Multiphysics

COMSOL Multiphysics is a commercial software or a Computer Aided Engineering (CAE) system for mathematical modeling. It is a technology that is based, among others, on the analysis of finite element methods (FEM). The software is intended to obtain approximate solutions of problems governed by ordinary and partial differential equations in multiphysics.

The division of the model into geometries facilitates the modeling of problems involving non-homogeneous domains, where physical properties vary as a function of spatial coordinates. Thus, the domain of a complex problem is discretized in several smaller and simple elements with the help of meshes of different types adapted to these geometries. COMSOL Multiphysics is a tool widely used in industry and has been growing in academia.

In our study model, the domains will be the layers in prismatic geometric shapes: air, oceanic structure and subsurface (formed by three layers: isotropic, anisotropic and basement). In the anisotropic layer, three resistive blocks (anomalies) with different sizes and resistivities simulate hydrocarbon reservoir and saline structure scenarios.

Open-source 3D Direct Modeling

Currently, four open-source codes stand out in numerical modeling in EM geophysics, which are in alphabetical order: custEM (Rochlitz et al., 2019); emg3d (Werthmüller et al., 2019); PETGEM (Castillo-Reyes et al., 2018, 2019) and SimPEG (Cockett et al., 2015; Heagy et al., 2017). All four codes have their user-facing routines written in Python, and they all make

intensive use of the NumPy packages (Harris et al., 2020) and SciPy (Virtanen et al., 2020).

All four follow the open development model, which means they come with an open-source license and an online hosted version control system with tracking possibilities (raising issues, filing pull requests). All developments comprise extensive online documentation with many examples and have continuous integration to some extent. Newer package management systems like Conda, Docker or pip make it simple to install all these codes on any major operating systems (Linux, MacOs, Windows).

In our work we will use the emg3d program. This code has an extensive documentation (Werthmüller et al., 2019) and examples, in addition to being the benchmark of our work compared to COMSOL Multiphysics. It uses the finite volume technique to solve the differential equation that governs numerical modeling and the multigrid method as the solver of the linear system.

METHODOLOGY

The geoelectric model analyzed in this work is an adaptation of the *Dublin Test Model 1* magnetotelluric (MT) method (Miensopust et al., 2013). This adaptation was elaborated by Werthmüller et al. (2021) and will be called the *block model*. In it, there are five layers and three blocks. The layered model (1D) consists of an upper half-space of air ($\rho_{air} = 1 \times 10^8\,\Omega\,m$), a 600 m-deep-water layer ($\rho_{sea} = 0.3\,\Omega\,m$), a 250 Ω m-thick isotropic layer with a resistivity of 1 Ω m, a 2.3 km-thick anisotropic layer (vertical transverse isotropy - VTI) with $\rho_h = 2\,hom\,m$ and $\rho_v = 4\,\Omega\,m$, and finally a resistive and isotropic basement consisting of a semi-bottom space of 1000 Ω m. The three blocks have equal resistivity of 500 Ω m, 10 Ω m and 100 Ω m. Figure 2 illustrates this model.
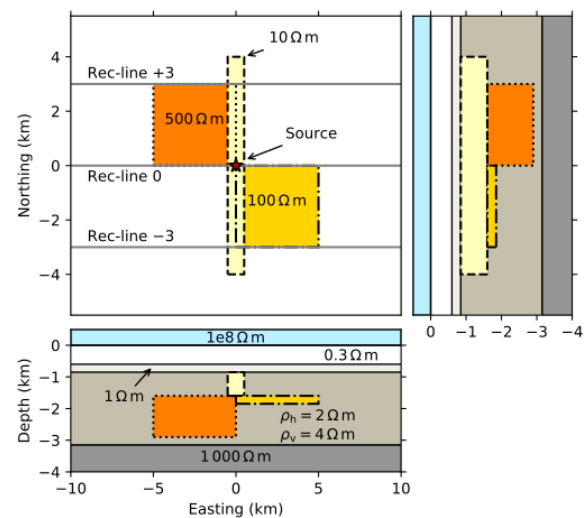

Figure 2: Block model, consisting of the background stratified and three blocks. (Adapted from Werthmüller et al., 2021).

Its construction and simulations of the MCSEM method were done using COMSOL Multiphysics and the open-source `emg3d` code (Werthmüller et al., 2019), as we will see below.

Building of the Model in COMSOL Multiphysics

COMSOL Multiphysics is a simulation and analysis software for numerous physical problems and applications in the field of engineering, which uses the finite element method as a numerical method. It includes a complete environment to model various physical phenomena that can be described using ordinary differential equations (ODE) or partial differential equations (PDE). The main advantages of this software are the friendly interface and the use of solvers optimized for the solutions of linear equations. There are many applications of COMSOL Multiphysics in numerical modeling, which can be accessed at the software web page. We can mention examples in geosciences, such as groundwater modeling (Li et al., 2009), and more specifically in applied modeling of electromagnetic methods (Butler and Zhang, 2016). Specifically for modeling the MCSEM and MT methods, we can cite the works of Leite and Tocantins (2015), Miranda and Tocantins (2017) and Li and Butler (2021).

The simulation work in COMSOL Multiphysics for the synthetic model presented in Figure 2 uses specifically the radio frequency (RF) module and the frequency domain interface. In this interface, simulations of the propagation/diffusion of electromagnetic waves are performed in the frequency domain from the numerical solution of the wave equation for the electric field (Pryor, 2022). For a better understanding, the simulation performed in COMSOL Multiphysics was divided into 3 steps: Step 1: Definition of model geometry and material; Step 2: Imposition of boundary conditions on the model; and Step 3: Domain Discretization.

Geometry and Material Definition: Step 1

Each layer of the block model is composed of a material with certain physical properties which, in the case applied to EM geophysics represent the electrical resistivity/conductivity, the dielectric permittivity and the magnetic permeability of the set of rocks and fluids. For each material that makes up the model, the user defines its properties in a geometric domain. Among the three physical properties relevant to EM geophysical methods, the main one is the electrical resistivity/conductivity. This is true in this work, because the geoelectric model, represented in Figure 2, does not take into account variations in the magnetic permeability and the dielectric permittivity of rocks and fluids, since, in the MCSEM method, the frequencies used are very low, in the order of tenths to a few hertz, and also because the geological environments where the method is employed are considered non-magnetic. In the following simulations, we will always convert the value of electrical resistivity to electrical conductivity.

The layered model built in the simulations is approximately 20 km wide (x-axis), 10 km deep (y-axis) and 3.9 km high (z-axis). The layer representing the air is 0.5 km thick; the sea water one is 0.6 km deep; the isotropic layer below is 0.25 km thick; the layer with anisotropy has a vertical dimension of 2.3 km; and the resistive basement is 0.25 km thick, as illustrated three-dimensionally in Figure 3.
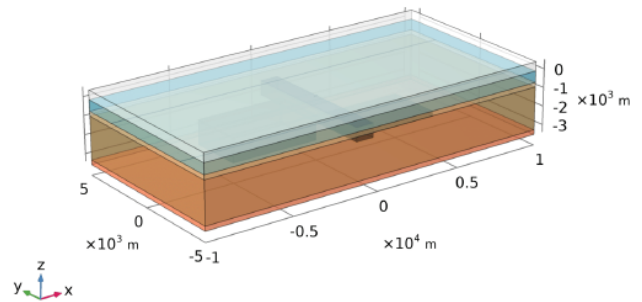

Figure 3: Three-dimensional view of the block model domain layers.

In the geoelectric model, blocks B1, B2 and B3 represent resistive targets and can be correlated to a high resistivity saline dome (B1: 500 Ω m), a reservoir with low resistivity (B2: 10 Ω m) and high resistivity reservoirs (B3: 100 Ω m). Block B1 is to the northwest, block B2 is in the middle and block B3 is to the southeast. The dimensions of these blocks are indicated in Table 1.

Table 1: Dimensions of Blocks B1, B2, and B3.

	B1	B2	B3
Width (km)	5.00	1.00	5.00
Depth (km)	3.00	8.00	3.00
Height (km)	1.30	0.75	0.25

A more detailed view of these blocks, already discretized in tetrahedral meshes generated by COMSOL Multiphysics, is represented in Figure 4. They are positioned within the anisotropic layer. The top view of these resistive blocks is shown in Figure 5.

The next step is to define the characteristics of the source and the receivers. The source is a horizontal electric dipole with a length of 200 m; it is located 50 m above the ocean floor. The receivers are at the ends from one side to the other ($x = -10$ km to $x = 10$ km), on $y = +3$ km, $y = 0$, and $y = -3$ km axes and at $z = 600$ m. So, we have three lines of receivers, one line located on the same axis as the direction of the source dipole, Rec-line 0, which is called

In-Line or radial array, and the other two lines of receivers Rec-line +3 and Rec-line −3, which are denoted as Broadside or Azimuthal array, illustrated in Figure 2. The receivers are distributed from −200 m to 200 m in the x directions of the three survey lines.
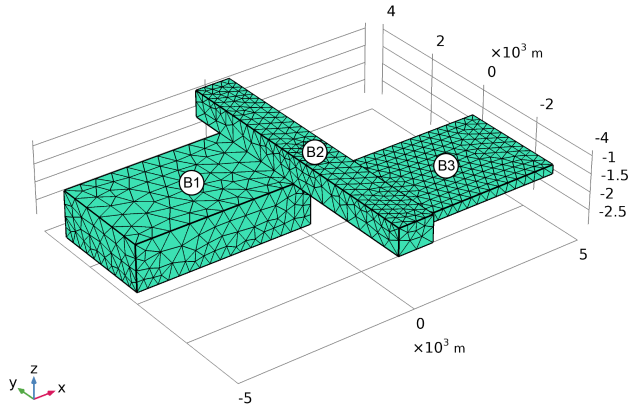

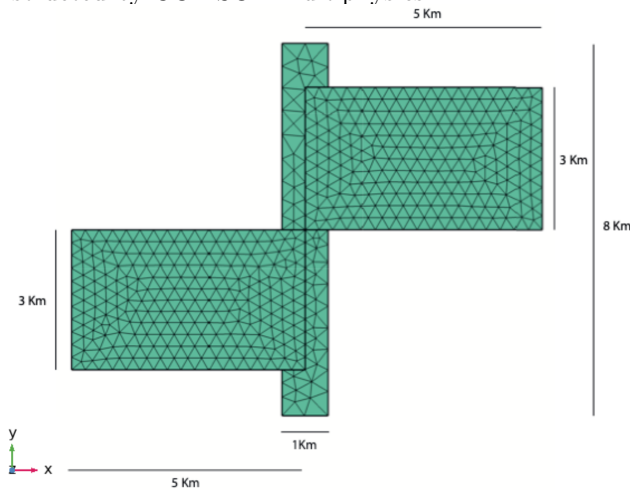Figure 4: Mesh of the three resistive blocks constructed by COMSOL Multiphysics.

Figure 5: Top view of the three resistive blocks, with their dimensions in x and y.

The electromagnetic properties of the materials characterized by COMSOL are: electrical conductivity (σ), reciprocal resistivity ($\sigma = 1/\rho$), dielectric permittivity (ε) and magnetic permeability (μ). The electrical conductivity is the capacity of the material to conduct electric current; its unit of measurement is the siemens per meter (S/m). The dielectric permittivity corresponds to the ability of a material to polarize in the presence of an electric field; its unit of measurement is farad per meter (F/m), while the magnetic permeability of a material is related to its ability to be magnetized in the presence of a magnetic field; its unit of measurement is henry per meter (H/m). Both the dielectric permittivity and the magnetic permeabilities can be normalized by reference values of these properties in the free space, namely the dielectric permittivity in free space, denoted by $\varepsilon_0 = 8.854 \times 10^{-12}$ F/m, and the magnetic permeability in free space, denoted by $\mu_0 = 4\pi \times 10^{-7}$ H/m.

Thus, in COMSOL, the values of the dielectric and magnetic properties of materials are relative to their values in free space and are represented by the relative electric permittivity ($\varepsilon_r = \varepsilon/\varepsilon_0$) and the relative magnetic permeability ($\mu_r = \mu/\mu_0$). As they are generally non-magnetic and non-dielectric in MCSEM method operating enviroments, $\mu = \mu_0$ and $\varepsilon = \varepsilon_0$. For our three-block model, we will always have ($\mu_r = 1$) and ($\varepsilon_r = 1$) for the horizontal layers or stratified medium and also for the resistive blocks B1, B2 and B3, or anomalies. Table 2 shows these values for both COMSOL and emg3d simulations.

Table 2 represents all the physical properties used in the model. As we saw earlier, for the marine geological environment where the MCSEM method is used, there is a very small variation in both the magnetic permeability and the dielectric permittivity of rocks and fluids in relation to their values in free space, that is, we can consider relative electrical permittivity and magnetic permeability values equal to 1.0 for the entire model. The table shows that the five layers have the following conductivities: the air layer (air) has a conductivity of 1×10^{-8} S/m; the ocean (sea) layer, 3.33 S/m; the isotropic layer (iso), 1.0 S/m; the anisotropic layer (ani) has its horizontal electrical conductivity (σ_h) equal to 0.5 S/m and its vertical (σ_v) one equal to 0.25 S/m. This type of anisotropy is known as vertical transverse isotropy (VTI). layer to layer (Régis and Santos, 2017). When building the model in COMSOL, we used an anisotropy matrix with the diagonal values $\sigma_{xx} = \sigma_{yy} = \sigma_h$ and $\sigma_{zz} = \sigma_v$.

Imposition of Boundary Conditions to the Model: Step 2

Before starting the next topic of mesh discretization, it is necessary to present the essential conditions for simulation models where the antenna or EM energy source is relatively close to the model boundaries.

In a desirable electromagnetic numerical modeling, the domain boundary would be open to infinity, that is, the wave transmitted through the dipole source would follow its propagation until its energy practically disappears. Of course, we cannot simulate an open boundary to infinity, but we can add boundary conditions to simulate this condition in the modeling.

COMSOL Multiphysics presents several ways to impose various types of boundary conditions. In geophysical modeling problems, where the scale of the models is on the order of tens of meters to tens of kilometers, we usually apply the Scattering Boundary Condition or Perfectly Matched Layer (PML). The scattering boundary condition causes the outer boundary of the computational domain to act as a transparent surface for scattered waves and also for incident plane waves, i.e., these boundaries must be far enough away from both incident waves and waves

Table 2: Material properties of layers and blocks B1, B2 and B3.

	Layers					Block		
	Air	**Sea**	**Iso**	**Ani**	**Emb**	**B1**	**B2**	**B3**
Electric conductivity (S/m)	10^{-8}	3.3	1.0	$\sigma_h = 0.50$ $\sigma_h = 0.25$	10^{-3}	10^{-3}	10^{-3}	10^{-3}
Relative permittivity (F/m)	1.0	1.0	1.0	1.0	1.0	1.0	1.0	1.0
Relative permeability (H/m)	1.0	1.0	1.0	1.0	1.0	1.0	1.0	1.0

scattered across them. Anomalies from waves arriving at the boundaries are considered normal to those boundaries (Huray, 2009). This leads to a much larger domain of the model, which is often an impediment for building in computers with little RAM. One way to get around this limitation and computational effort is to use a layer outside the model domain, that absorbs the scattered and incident waves, being achieved with the use of the PML.

The Perfectly Matched Layer works similarly to an infinity boundary and is mainly added if the model contains an air layer. In order to have a more accurate simulation, this condition will add a new region, or rather, a half-space around the finite model and, thus, the radiated waves can propagate, being strongly absorbed with minimal or no reflection, preventing them to return inside the domain where the receivers are deployed. The PML methodology (Pryor, 2022; Johnson, 2021) works by adding these anisotropic attenuating domains (layers) outside the modeled domain. The anisotropic attenuating domains create an essentially unreflected set of boundaries for the modeled domain. The construction of this type of boundary is illustrated in Figure 6.
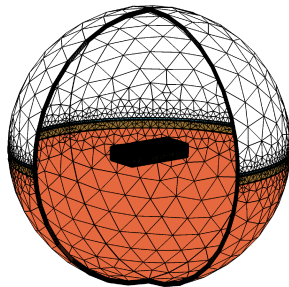

Figure 6: Perfectly absorbing PML layer used in the model. Note that the discretization elements are hexahedrons and do not belong to the in-domain of the model.

In COMSOL, there are four types of PML configuration. We used the spherical configuration due to the symmetry of our type of source (electric dipole).

Domain Discretization: Step 3

Figures 2, 5 and 6 illustrate meshes in blocks B1, B2 and B3 and the implementation of the boundary condition via PML. However, some factors that determine a suitable discretization for the simulation in COMSOL Multiphysics are build throughout meshes for each subdomain of the model. The meshes are characterized by a set of nodal points, together with the characteristics of the finite elements that form the discretization of the modeling domain. There are nine default mesh sizes in the COMSOL software; we handle with three types of these. Depending on the size and geometric shape of the three-dimensional bodies, we can have a certain discretization of the subdomains for the simulation in COMSOL. Bodies or, in our case, blocks must have a greater discretization than large subdomains, such as the air layer and the basement. Also, domains where primitive objects represent an electromagnetic source, such as the horizontal electric dipole and receivers of measurements of the electric and magnetic fields, must have a very dense discretization around these points. This is necessary due to the wide variation of EM fields close to the source and also for the reason that these electromagnetic fields are often obtained by interpolating the values of other EM fields or EM potentials around the receivers. COMSOL does all this analysis automatically, when we opt for the free mesh, but user intervention is always necessary in the simulation, which must take into account where measurements are evaluated, the representation of the source and most importantly the computational capacity of the system in use. Mesh construction has a bit of art. The more refined it is, the more accurate it is, and more elements are created from an original domain. However, extremely fine meshes require more memory and processing time. So, we must be judicious in its construction. Table 3 shows the sizes of the predefined refinements of the meshes built for the layers

Table 3: Mesh discretization of the layers and the blocks.

	Air	**Sea**	**Iso**	**Ani**	**Emb**	**B1**	**B2**	**B3**
Slim	✓				✓			
Extra Thin		✓	✓	✓				
Extremely Thin						✓	✓	✓

and blocks of the studied model and the Figure 7 illustrates the various levels of refinements employed to build the model.
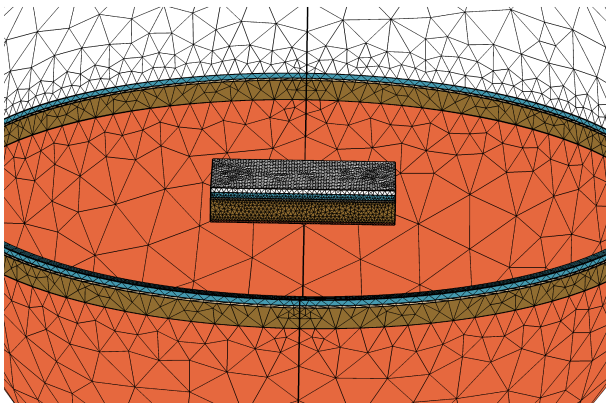

Figure 7: Discretization of the layers and the region where blocks B1, B2 and B3 are found.

THE emg3d CODE

We followed the description of Werthmüller et al. (2021) of the emg3d code for modeling the controlled-source electromagnetic method, where it presents itself as a multigrid type solver (Fedorenko, 1964) applied to electromagnetic diffusion with the particularity of including triaxial electrical anisotropy (Mulder, 2006). The matrix free solver can be used as the main solver or as a preconditioner for one of the Krylov subspace methods implemented in SciPy.

The governing equations are discretized in a scaled grid by the finite integration technique (Weiland, 1977), which is a generalization of the finite volume method of a Yee grid. The code is written completely in Python using the NumPy and SciPy packages, where the most consuming parts of time and memory are accelerated through *jitted* functions (compiled just-in-time) using Numba (Lam et al., 2015).

The advantage of emg3d is the matrixless multigrid implementation, which is characterized by a quasi-linear scaling in terms of both runtime and memory usage, being therefore a solver that uses comparatively less memory than, for example, COMSOL Multiphysics. The code is primarily a solver, which computes Maxwell's equations for a single frequency from a single electrical source. Recent developments have added functionality to the emg3d code, which

can also be used directly as a more general EM modeler (Werthmüller et al., 2021).

In addition to the functionality to model arbitrarily directed electrical sources and receivers, the emg3d code can also simulate magnetic sources and receivers, as well as model time-domain responses. The code has routines for getting the gradient of the misfit function that can be used by inversion algorithms. The discretization of the emg3d code is done by the Python discretize package, which is part of a larger ecosystem called SimPEG (Cockett et al., 2015).

RESULTS

In this section we present the results of the simulations using the emg3d code and COMSOL Multiphysics. We will analyze in a first approach a comparison of the results of the two simulations and then we will present other scenarios of interest in the MCSEM method using these two codes.

In this research, a single hardware setup was used for simulations. The desktop computer used had a Windows operating system, an Intel i5 processor, and 16 GB of RAM. The simulations were carried out using the COMSOL Multiphysics software. The emg3d code, developed in Python, was run on the same computer using the open-source Anaconda distribution platform (Anaconda Software Distribution, 2021) and the Jupyter Notebooks development environment.

A comparison between the two methodologies used in the simulations is presented in Table 4. The tetrahedral finite element method used by COMSOL Multiphysics results in longer processing times compared to the hexahedral finite volume numerical method used by the emg3d code, although this may vary depending on the specific problem being simulated. Additionally, emg3d uses less memory, as a greater number of tetrahedral finite elements are required to accurately discretize the same domain discretized by hexahedrons.

Simulations with COMSOL Multiphysics Versus emg3d

The results of these tests show that, in the simulated conditions, the finite volume (emg3d) and finite element methods (COMSOL) present small differences. The magnitude of the electric field obtained by COMSOL differs partially from that simulated by emg3d at the ends of the graph, that is, close to the boundaries

Table 4: Comparison between COMSOL and `emg3d` based on different technical specifications and requirements.

Specifications	COMSOL	emg3d
Numerical method	Finite elements	Finite volumes
Mesh Type	Tetrahedron	Hexahedron
Processing time (s)	1246	194
Used memory (GB)	0.8	0.41
License	Commerce	Apache 2.0

of the model. However, for small offsets, the convergence between them is satisfactory. For example, in Figure 8 we can see that between -5 km to 5 km the convergence between the simulations between the two approaches is quite pronounced, differing approximately between -6 km to -10 km and between 8 km to 10 km.
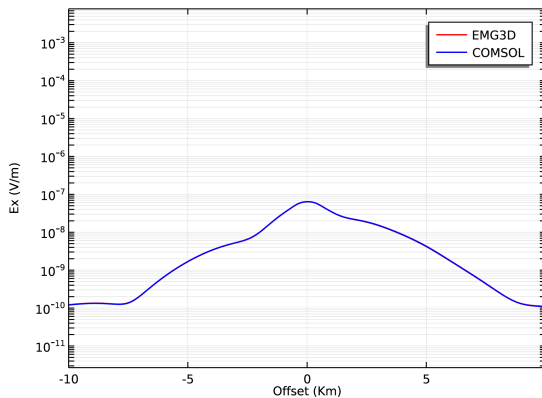
Figure 8: Comparison of electric field amplitudes (E_x) along the Broadside receiver line at $y = -3$ km.

Comparisons of the simulation results along the other acquisition lines also demonstrate this consistency. Figure 9 shows the amplitudes of the electric field E_x, in the *in-line* geometry ($y = 0$ km), that is, in the line the receivers pass below the transmitter in the same direction (x) of the electromagnetic source.
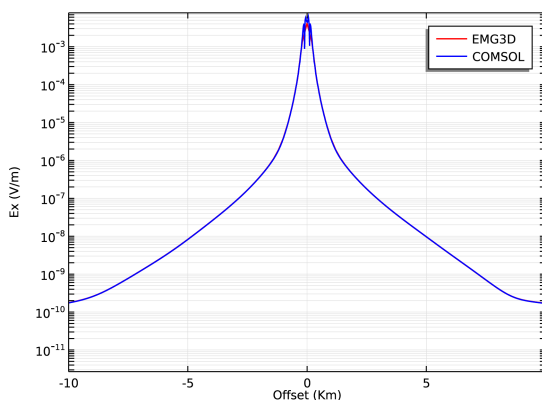
Figure 9: Comparison of electric field amplitudes (E_x) along the In-Line receiver line at $y = 0$ km.
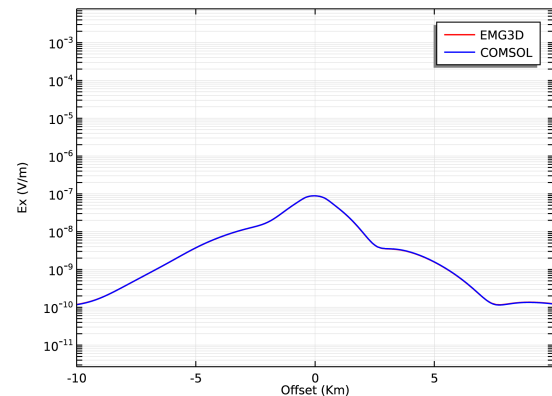
Figure 10: Comparison of electric field amplitudes (E_x) along the Broadside receiver line at $y = +3$ km.

The Figure 10 shows the amplitude of the electric field E_x in the Broadside geometry at $+3$ km. That is, the receivers are in the direction of the electromagnetic source, x direction, but away from $y = +3$ km. Note the antisymmetry of the curves in Figure 8. Differences in amplitudes situated close to the limits of the model can be caused by two factors. First, simply because they are different methods, where each one uses different representations for variables to round off values with a certain numerical precision. Second, numerical techniques have different numerical accuracies and getting small differences in the results obtained is natural. For example, it is known that the finite element method is more suitable for complex geometries, despite consuming more machine memory. Finite volume methods are used with great success in rectangular geometries, as it is the case of our block model. However, the representation of a point source, such as the horizontal electric dipole, is still a challenge for a better representation in this method. Another very important factor is the implementation of the boundary condition by PML. We did the trial and error method until we had a result as close as possible. The result without the PML was completely different; it was clear the interference of incident and reflected waves in the layer, increasing consequently the magnitude of the field around it. In particular, the antisymmetry characteristics were conserved. For example, in Broadside -3 km and Broadside $+3$ km, electric fields have opposite behavior to each other,

although the mesh is not symmetric for COMSOL and the model body is horizontally antisymmetric, with a small difference in thickness of block B3 (Figures 2 and 3), since it is thinner (0.25 km) than block B1 (1.3 km). This means that the method is robust enough and does not depend on mesh discretization. It can be considered that the answer is getting validated. It is important to point out that the frequency used in this comparison was 1.0 Hz and the source current was 800 A, being, therefore, the same used in the work of Werthmüller et al. (2021).

Comparing Anomalies

After validating the simulations with COMSOL Multiphysics and `emg3d`, we have a powerful tool available for electromagnetic modeling of the MCSEM method and with that we can do more complete analyses using the same data with some modifications or specific situations. As in the case of this same three-block model, we can simulate models with and without the presence of these three resistive bodies and thus carry out a study and analysis in greater detail. When we analyze in terms of anomalies in the middle of the background, we can visualize the effect of the energy transmitted through the 200-meter-long dipole source located in the center of the model with its ends at $x = -100$ m and $x = +100$ m. The electromagnetic fields propagate in the background layers and part of them is reflected from the resistive blocks until they reach the receivers where the data will be measured, resulting in a received signal greater than it would be if these blocks were not present. This effect is shown in the next three graphs where the electric field E_x is plotted as a function of distance for situations with resistive blocks (blue line), denoted Block Model because it represents possible anomalies related to the presence of resistive blocks. The green line represents the background, that is, only the one-dimensional stratified model, or background model, which we will call Background. The Figure 11 presents the amplitudes of the electric fields in the x direction for the presence/absence of the resistive blocks. The acquisition line is Broadside -3 km, i.e., the distance in y from the source is -3 km. We observed that the receptors close to block B3 strongly detect the resistive body (blue line - Block Model), where block B1 is located. In the case of the In-Line acquisition line, Figure 12, where $y = 0$ km, we observe the difference in the curves of the electric fields E_x in realation to the presence of the resistive blocks. This is the characteristic curve of a survey of the MCSEM method. The graph in Figure 12 shows that the receivers which are under the source present many oscillations, as a result of the punctual nature of the source and the proximity of the receiver to the dipole, which makes the translation to a numerical instability in the calculations of the electric fields. Figure 13 illustrates the simulations for the E_x field on the Broadside receiver line at $y = +3$ km. Note the anomaly on the left side

of the graph. Figures 11 and 13 have anti-symmetric shapes, but they are different. The reason is due to the symmetry of the arrangement of the bodies, which have different thicknesses and resistivities.
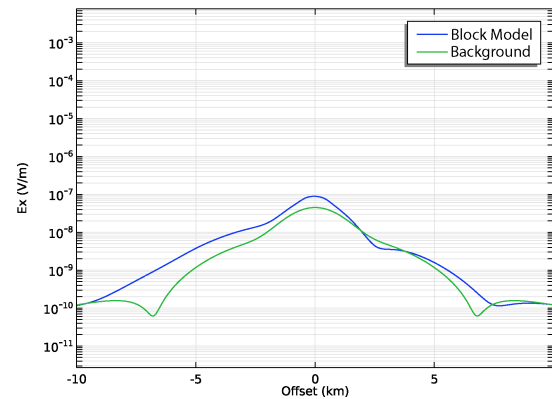

Figure 11: E_x Broadside electric field amplitudes at y = -3 km. The blue line represents the model containing the resistive blocks; the green line represents the "Background".
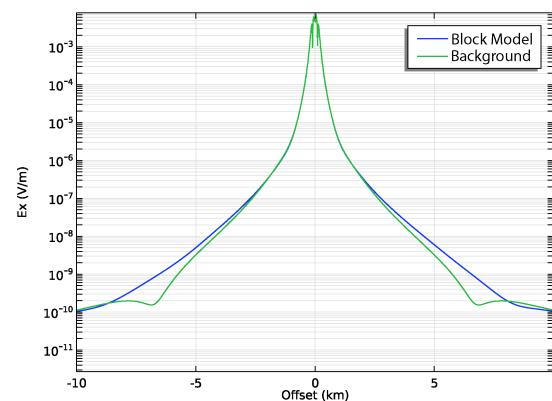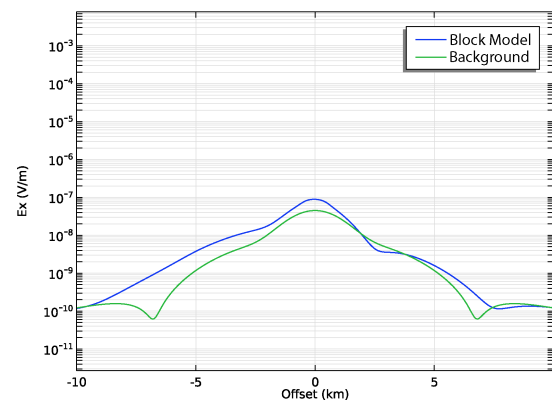

Figure 12: E_x In-Line electric field amplitudes. The green and blue lines represent respectively the answers of the "Backgroud" and "Block Model".

Figure 13: E_x Broadside electric field amplitudes at y = $+3$ km. The blue line represents the model containing the resistive blocks; the green line represents the "Background".

Simulations in Multifrequency

Studying multiple frequencies or multifrequency is useful to get more information about how resistivity is distributed in the subsurface. It is important for MCSEM as it will help to better delineate a reservoir and, thus, could become an important complement to exploration seismic. Operating frequencies for the MCSEM method range from tenths of a Hz to a few units of Hz depending on the possible resistive targets and the environment surrounding these targets. Figure 14 presents the curves of the electric field amplitudes in the x-direction for the Broadside acquisition line at $y = -3$ km. We used six frequencies in the simulations with COMSOL Multiphysics. We noticed that the higher the frequency, the smaller its range, that is, the smallest depth the electromagnetic wave can detect targets, which is the skin-depth effect. The curves in Figure 14 demonstrate this feature. The E_x field at the frequency of 1.25 Hz has a much smaller amplitude than the E_x field operating at 0.125 Hz, but we observed that the curve at 1.25 Hz has a higher resolution than that obtained at 0.125 Hz.
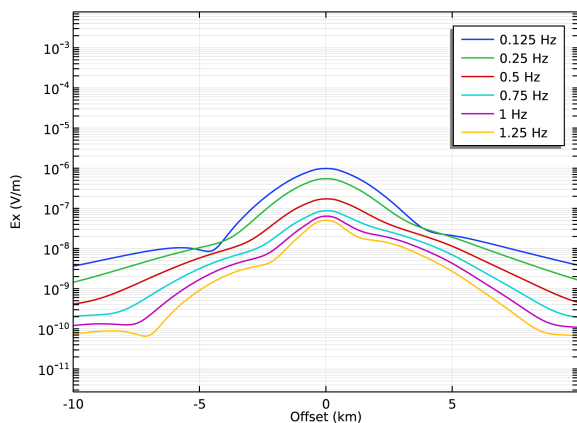

Figure 14: E_x Broadside electric field amplitudes at $y = -3$ km in multifrequency.

The multifrequency fields in the In-Line configuration are illustrated in Figure 15.
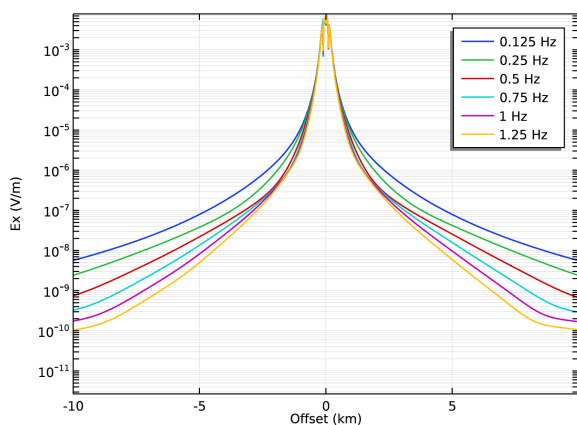

Figure 15: E_x In-Line electric field amplitudes at $y = 0$ km in multifrequency.

In the same way, as seen before, we observed that the higher the frequency, the smaller the field amplitude. Figure 16 shows the E_x field amplitudes in the Broadside acquisition at $y = +3$ km, at the same frequencies as the other acquisitions. We observed that for just one frequency we could confuse it with a perfect antisymmetry in the Broadside surveys and have the clear impression that blocks B1 and B3 are identical. We now see, comparing Figures 14 and 16, a notable difference in the fields, mainly in the high frequencies.
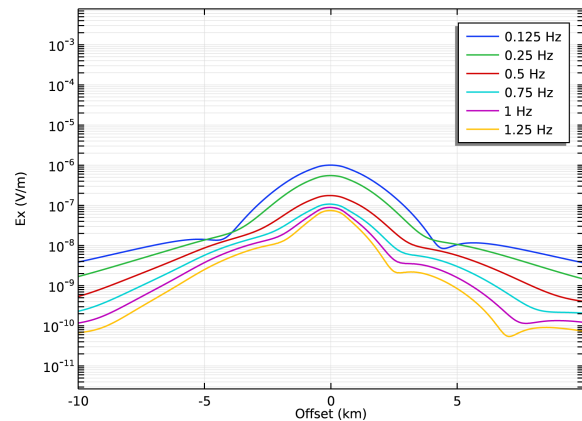

Figure 16: E_x Broadside electric field amplitudes at $y = +3$ km in multifrequency.

CONCLUSIONS

In this work, we simulate the MCSEM method for a resistive block model applying two different approaches: in the first one, we use COMSOL Multiphysics and in the other we use the `emg3d` code. Working with different numerical methodologies in the solution of electromagnetic problems in geophysics has always been a reason for discussions, due to the relationship between the numerical methodologies of greater computational effort, as in the case of the finite element and the intrinsic resolution of electromagnetic methods that being related to a diffusion phenomenon provide lower resolution than the one for the wave propagation phenomenon. Thus, in 3D modeling, integral methods and finite differences have taken preferences in the solution of EM problems. With the decrease in computational cost (memory) and increase in processing speed, methods that explore a greater refinement in geoelectrical model geometries have been developed and improved, as well as their algorithms and numerical techniques in the solution of linear systems and approximations of integral representations of the electromagnetic fields. The results obtained in the comparison of these two approaches were mainly consistent in small offsets in relation to the source. We also observed a difference in the electric field curves in the two simulation models (COMSOL Multiphysics and `emg3d`): close to the model domain boundaries, it is deserved studies and

analysis on the influence of boundary conditions and methods for impedance matching, as well as reflection absorption methodologies, as it is the case with the use of the technique of infinite elements in the boundary regions of the domain. It has been shown that although COMSOL Multiphysics requires a greater computational effort, its intuitive interface and easy interaction with other model building and modeling tools, for example, MATLAB and CAD, are the great attractions of its use despite being a commercial software. It is worth mentioning the speed of the solvers optimized for the COMSOL system of linear equations. This is a topic of constant discussion and development in any large-scale numerical technique. For the `emg3d` code, it was exposed that it is easy to use it for models of simple geometries. The code proved to be efficient, easy to use and simple to install through the *Conda* package manager. The code is intended for use in quick feasibility analysis of exploration scenarios and also for learning and research at the academy, for having its source code available. With wide dissemination of its applications and development with other open-source EM modeling programs around the world, the `emg3d` code undoubtedly has a relevant role in modeling research on electromagnetic methods.

ACKNOWLEDGMENTS

REFERENCES

Anaconda Software Distribution, 2021, Computer software, vers. 2021.11: https://anaconda.com.

Butler, S. L., and Z. Zhang, 2016, Forward modeling of geophysical electromagnetic methods using comsol: Computers & Geosciences, **87**, 1–10, doi: 10.1016/j.cageo.2015.11.004.

Castillo-Reyes, O., J. de la Puente, and J. M. Cela, 2018, PETGEM: A parallel code for 3D CSEM forward modeling using edge finite elements: Computers & Geosciences, **119**, 123–136, doi: 10.1016/j.cageo.2018.07.005.

Castillo-Reyes, O., J. de la Puente, L. E. García-Castillo, and J. M. Cela, 2019, Parallel 3-D marine controlled-source electromagnetic modelling using high-order tetrahedral Nédélec elements: Geophysical Journal International, **219**, 39–65, doi: 10.1093/gji/ggz285.

Chave, A. D., S. C. Constable, and R. N. Edwards, 1991, Electrical exploration methods for the seafloor, *in* Electromagnetic Methods in Applied Geophysics: Volume 2, Application, Parts A and B: Society of Exploration Geophysicists, 931–966. doi: 10.1190/1.9781560802686.ch12.

Chave, A. D., and C. S. Cox, 1982, Controlled electromagnetic sources for measuring electrical conductivity beneath the oceans: 1. Forward problem and model study: Journal of Geophysical Research, **87**, 5327–5338, doi: 10.1029/JB087iB07p05327.

Chave, A. D., and C. S. Cox, 1983, Electromagnetic induction by ocean currents and the conductivity of the oceanic lithosphere: Journal of Geomagnetism and Geoelectricity, **35**, 491–499, doi: 10.5636/jgg.35.491.

Cockett, R., S. Kang, L. J. Heagy, A. Pidlisecky, and D. W. Oldenburg, 2015, SimPEG: An open source framework for simulation and gradient based parameter estimation in geophysical applications: Computers & Geosciences, **85**, 142–154, doi: 10.1016/j.cageo.2015.09.015.

Constable, S., 1990, Marine electromagnetic induction studies: Surveys in Geophysics, **11**, 303–327, doi: 10.1007/BF01901663.

Edwards, N., 2005, Marine Controlled Source Electromagnetics: Principles, Methodologies, Future Commercial Applications: Surveys in Geophysics, **26**, 675–700, doi: 10.1007/s10712-005-1830-3.

Eidesmo, T., S. Ellingsrud, L. MacGregor, S. Constable, M. Sinha, S. Johansen, F. Kong, and H. Westerdahl, 2002, Sea Bed Logging (SBL), a new method for remote and direct identification of hydrocarbon filled layers in deepwater areas: First Break, **20**, doi: 10.3997/1365-2397.20.3.25008.

Ellingsrud, S., T. Eidesmo, S. Johansen, M. Sinha, L. MacGregor, and S. Constable, 2002, Remote sensing of hydrocarbon layers by Seabed Logging (SBL): Results from a cruise offshore Angola: The Leading Edge, **21**, 972–982, doi: /10.1190/1.1518433.

EMGS, 2022, Controlled Source Electromagnetics (CSEM): EMGS, Available on: https://emgs.com/technology/a-guide-to-marine-em/csem.

Fedorenko, R., 1964, The speed of convergence of one iterative process: USSR Computational Mathematics and Mathematical Physics, **4**, 227–235, doi: 10.1016/0041-5553(64)90253-8.

Harris, C. R., K. J. Millman, S. J. van der Walt, R. Gommers, P. Virtanen, D. Cournapeau, E. Wieser, J. Taylor, S. Berg, N. Smith, R. Kern, M. Picus, S. Hoyer, M. H. van Kerkwijk, M. Brett, A. Haldane, J. F. del Río, M. Wiebe, P. Peterson, P. Gérard-Marchant, K. Sheppard, T. Reddy, W. Weckesser, H. Abbasi, C. Gohlke, and T. E. Oliphant, 2020, Array programming with NumPy: Nature, **585**, 357–362, doi: 10.1038/s41586-020-2649-2.

Heagy, L. J., R. Cockett, S. Kang, G. K. Rosenkjaer, and D. W. Oldenburg, 2017, A framework for simulation and inversion in electromagnetics: Computers & Geosciences, **107**, 1–19, doi: 10.1016/j.cageo.2017.06.018.

Huray, P. G., 2009, The foundations of signal integrity: John Wiley & Sons, Inc.

Johnson, S. G., 2021, Notes on perfectly matched layers (PMLs): CoRR, **abs/2108.05348**, doi: 10.48550/ARXIV.2108.05348.

Lam, S. K., A. Pitrou, and S. Seibert, 2015, Numba: A LLVM-Based Python JIT Compiler, *in* Proceedings of the Second Workshop on the LLVM Compiler Infrastructure in HPC, Austin Texas: Association for Computing Machinery, LLVM'15. doi: 10.1145/2833157.2833162.

Leite, M. L., and V. C. Tocantins, 2015, Modelagem tridimensional do método MCSEM usando COMSOL Multiphysics, *in* 14th International Congress of the Brazilian Geophysical Society; EXPOGEF, Rio de Janeiro, Brazil, 3-6 August 2015: Society of Exploration Geophysicists, 197–199. doi: 10.1190/sbgf2015-039.

Li, A., and S. Butler, 2021, Forward modeling of magnetotellurics using COMSOL Multiphysics: Applied Computing and Geosciences, **12**, 100073, doi: 10.1016/j.acags.2021.100073.

Li, Q., K. Ito, Z. Wu, C. S. Lowry, and S. P. Loheide II, 2009, COMSOL Multiphysics: A novel approach to ground water modeling: Groundwater, **47**, 480–487, doi: 10.1111/j.1745-6584.2009.00584.x.

Miensopust, M. P., P. Queralt, A. G. Jones, and the 3D MT modellers, 2013, Magnetotelluric 3-D inversion—a review of two successful workshops on forward and inversion code testing and comparison: Geophysical Journal International, **193**, 1216–1238, doi: 10.1093/gji/ggt066.

Miranda, H. D. T., and V. C. Tocantins, 2017, 2.5 marine CSEM modeling using COMSOL Multiphysics, *in* 15th International Congress of the Brazilian Geophysical Society; EXPOGEF, Rio de Janeiro, Brazil, 31 July-3 August 2017: Society of Exploration Geophysicists, 211–216. doi: 10.1190/sbgf2017-042.

Mulder, W., 2006, A multigrid solver for 3D electromagnetic diffusion: Geophysical Prospecting, **54**, no. 5, 633–649, doi: 10.1111/j.1365-2478.2006.00558.x.

Pryor, R., 2022, Multiphysics Modeling Using COMSOL 5 and MATLAB, 2 ed.: Mercury Learning and Information.

Rochlitz, R., N. Skibbe, and T. Günther, 2019, custEM: Customizable finite-element simulation of complex controlled-source electromagnetic data: Geophysica, **84**, F17–F33, doi: 10.1190/geo2018-0208.1.

Régis, C., and W. Santos, 2017, Delineation of anisotropic layers through 1D inversion of marine CSEM data: Brazilian Journal of Geophysics, **34**, 543–558, doi: 10.22564/rbgf.v34i4.870.

Virtanen, P., R. Gommers, T. E. Oliphant, M. Haberland, T. Reddy, D. Cournapeau, E. Burovski, P. Peterson, W. Weckesser, J. Bright, S. J. van der Walt, M. Brett, J. Wilson, K. J. Millman, N. Mayorov, A. R. J. Nelson, E. Jones, R. Kern, E. Larson, C. J. Carey, İ. Polat, Y. Feng, E. W. Moore, J. VanderPlas, D. Laxalde, J. Perktold, R. Cimrman, I. Henriksen, E. A. Quintero, C. R. Harris, A. M. Archibald, A. H. Ribeiro, F. Pedregosa, P. van Mulbregt, A. Vijaykumar, A. P. Bardelli, A. Rothberg, A. Hilboll, A. Kloeckner, A. Scopatz, A. Lee, A. Rokem, C. N. Woods, C. Fulton, C. Masson, C. Häggström, C. Fitzgerald, D. A. Nicholson, D. R. Hagen, D. V. Pasechnik, E. Olivetti, E. Martin, E. Wieser, F. Silva, F. Lenders, F. Wilhelm, G. Young, G. A. Price, G.-L. Ingold, G. E. Allen, G. R. Lee, H. Audren, I. Probst, J. P. Dietrich, J. Silterra, J. T. Webber, J. Slavič, J. Nothman, J. Buchner, J. Kulick, J. L. Schönberger, J. V. de Miranda Cardoso, J. Reimer, J. Harrington, J. L. C. Rodríguez, J. Nunez-Iglesias, J. Kuczynski, K. Tritz, M. Thoma, M. Newville, M. Kümmerer, M. Bolingbroke, M. Tartre, M. Pak, N. J. Smith, N. Nowaczyk, N. Shebanov, P. A. Pavlyk, Oleksandrv Brodtkorb, P. Lee, R. T. McGibbon, R. Feldbauer, S. Lewis, S. Tygier, S. Sievert, S. Vigna, S. Peterson, S. More, T. Pudlik, T. Oshima, T. J. Pingel, T. P. Robitaille, T. Spura, T. R. Jones, T. Cera, T. Leslie, T. Zito, T. Krauss, U. Upadhyay, Y. O. Halchenko, Y. Vázquez-Baeza, and SciPy 1.0 Contributors, 2020, SciPy 1.0: fundamental algorithms for scientific computing in Python: Nature Methods, **17**, 261–272, doi: 10.1038/s41592-019-0686-2.

Weiland, T., 1977, Eine Methode zur Lösung der Maxwellschen Gleichungen für sechskomponentige Felder auf diskreter Basis: International Journal of Electronics and Communications, **31**, 116–120.

Werthmüller, D., W. A. Mulder, and E. C. Slob, 2019, EMG3D: A multigrid solver for 3D electromagnetic diffusion: Journal of Open Source Software, **4**, 1463, doi: 10.21105/joss.01463.

Werthmüller, D., R. Rochlitz, O. Castillo-Reyes, and L. Heagy, 2021, Towards an open-source landscape for 3-D CSEM modelling: Geophysical Journal International, **227**, 644–659, doi: 10.1093/gji/ggab238.

Seabra, L.: COMSOL Multiphysics model development and implementation, simulations and result analysis; **Pires, H.**: `emg3d` model development and implementation, simulations and result analysis; **Penha, W.**: manuscript writing and formatting; **Monteiro, D.**: model development and implementation, result analysis; **Monteiro, A.**: manuscript writing and formatting, study design, result interpretation; **Tocantins, V.**: manuscript writing and formatting, study design, result interpretation.